# PMU-based power system analysis of a medium-voltage distribution grid

Save, Nishant; Popov, Marjan; Jongepier, Arjen; Rietveld, Gert

**DOI**
10.1049/oap-cired.2017.1035

**Publication date**
2017

**Document Version**
Final published version

**Published in**
CIRED - Open Access Proceedings Journal

24th International Conference & Exhibition on Electricity Distribution (CIRED)

12-15 June 2017

*Session 4: Distributed energy resources and active demand integration*

# PMU-based power system analysis of a medium-voltage distribution grid

ISSN 2515-0855
doi: 10.1049/oap-cired.2017.1035
www.ietdl.org

*Nishant Save*[1] ✉, *Marjan Popov*[1], *Arjen Jongepier*[2], *Gert Rietveld*[3]

[1]*Electrical Sustainable Energy, TU Delft, Delft, The Netherlands*
[2]*Sustainability and Innovation, Enduris, Goes, The Netherlands*
[3]*VSL – The Dutch National Metrology Institute. (Van Swinden Laboratory), Delft, The Netherlands*
✉ *E-mail: nishant_save@yahoo.com*

**Abstract:** The installation of phasor measurement units (PMUs) by Enduris, one of the distribution network operators in the Netherlands to monitor their 50 kV ring distribution grid has resulted in increased observability of the power flows and voltages. However, with the increased observability, there is a need to analyse the distribution grid based on the data generated by the PMU monitoring system. This study provides steady-state and dynamic analysis of the 50 kV Enduris ring distribution grid in terms of voltage and power flow behaviour based on the real-time data acquired from the PMUs. First, the Enduris 50 kV distribution grid under study is modelled in PowerFactory software. This model is subsequently used for analysis of the distribution grid behaviour for two contingencies. The contingencies are actual grid events observed by the PMUs, and using this data, the contingencies are simulated and analysed. The analysis results of each contingency are compared with the data from the PMU monitoring system.

## 1 Introduction

The need for a better distribution grid monitoring infrastructure due to increasing penetration of renewable energy sources has prompted Enduris (Delta Network Group is as per January 2016 renamed as Enduris, the name used in this paper.), one of the distribution network operators (DNOs) in the Netherlands, to install phasor measurement units (PMUs) in their 50 kV ring distribution grid. By this, an increased observability of their 50 kV distribution grid is achieved [1]. In [1], details about the need of using PMU infrastructure for monitoring the Enduris 50 kV distribution grid, the description of the 50 kV ring distribution network and the possible applications of PMUs in the distribution grid is provided.

This paper provides an analysis of behaviour of the Enduris distribution grid based on the power flow behaviour and the voltages in the 50/10/0.4 kV distribution grid by using the real-time data acquired from the PMU measurements. First, the Enduris 50 kV distribution grid is modelled in PowerFactory software. Subsequently, two grid contingencies, one in the 50 kV distribution grid and one in the 10/0.4 kV sub-distribution grid, are identified and described by making use of the PMU measurements.

Next, a methodology is described to calculate the approximate aggregated generation and load in the distribution grid using the real-time power flow values from PMU and supervisory control and data acquisition (SCADA) measurements. This methodology forms the basis for calculating the initial load flow condition during each of the grid contingencies.

From the simulation results, the power flow behaviour and voltages in the distribution grid are analysed and the response of the distributed generation (DG) is predicted during both events. The analysis results are compared with the actual PMU measurements and conclusions about the grid behaviour are drawn based on the studied contingencies.

## 2 Modelling of the 50/10/0.4 kV distribution grid

The network of the Enduris 50 kV distribution grid as shown in Fig. 1 and further described in paper [1] is modelled using PowerFactory software. The ring distribution grid consists of six sub-stations connected to each other via 50 kV cables (except for the Gsp-150 150 kV to goes evertsenstraat 50 kV substation (Gse)-50 50 kV substations which is a 50 kV line connection). The ring network is connected to the 150 kV parallel transmission lines through 150/50/10 kV three winding power transformers as shown in Fig. 1. The 150 kV transmission network is represented by an external infinite grid connected at the Gsp-150 150 kV substation modelled as a slack bus to perform power balancing of the distribution grid. This is an assumption of a 50 kV distribution grid containing DG set as *PQ* nodes, and the external grid acting as a reference bus providing grid balancing [2].

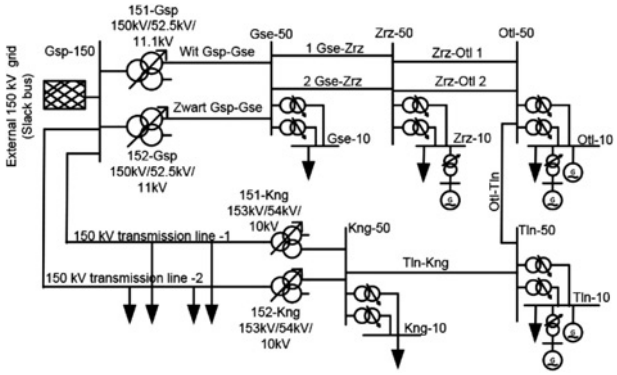


**Fig. 1** *Schematic Enduris 50 kV distribution grid model*

The analysis is concentrated on the five 50 kV substations of Gse, zierikzee 50 kV substation (Zrz), oosterland 50 kV substation (Otl), thoelen 50 kV substation (Tln) and kruinigen 50 kV substation (Kng) and their respective 10 kV bus, which form the 50 kV ring distribution grid monitored by PMUs. The connection between the 50 kV and its respective 10 kV bus is through parallel two winding 52/11.1 kV distribution transformers with only one transformer in service at a given time.

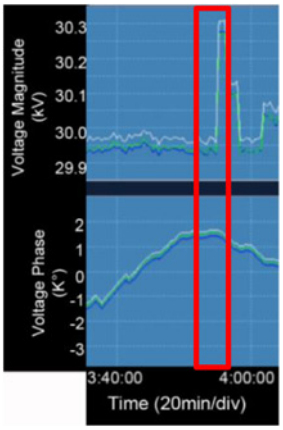


**Fig. 2** *PMU snapshot highlighting in red the change in voltage and voltage phase angle as a result of 50 kV overhead line disconnection at the Gse-50 50 kV substation*

Each of the 10 kV buses has a mix of DG and loads connected down to 0.4 kV voltage level. The DG consists a mix of wind farms and combined heat and power (CHP) plants. The DG sources at each of the 10 kV buses are modelled as single machine representation of total aggregated wind power and CHP plants.

For wind turbines, generic doubly fed induction generator (DFIG) models connected at 0.4 kV bus available in PowerFactory with pre-defined control parameters are used with a step-up transformer connecting the DFIG to the 10 kV bus [3]. The CHP plants are modelled as single machine synchronous generator directly connected to 10 kV bus and equipped with voltage control and speed governor control. The loads are modelled as general static constant impedance; inductive load with a voltage dependency [4] directly connected to the 10 kV bus. The approach similar to [5] is used here for similar distribution grid studies.

## 3 Event description based on PMU monitoring

### 3.1 Contingency in the 50 kV distribution grid

The contingency considered here is an actual event, namely the disconnection of one of the two overhead lines connecting the Gse-50 kV substation with the Gsp-150 substation (see Fig. 1).

The PMU measurements of the contingency are available in the form of snapshots from the PMU which monitors the Gse-50 kV substation.

The PMU snapshot of the contingency as shown in Fig. 2 shows the real-time variation of per phase voltage ($V_{ph}$ in kV) and the continuous voltage phase angle variation ($\delta$ in degrees) at the Gse-50 50 kV substation over a period of 20 min with the time instant of overhead line disconnection highlighted in red. As observed, the per phase voltage ($V_{ph}$ in kV) at the Gse-50 50 kV substation increases slightly from ~29.95 to 30.3 kV. For the purpose of the analysis, the distribution grid is considered as a balanced three-phase network; hence, the jump in voltage when calculated to three-phase line-to-line voltage ($V_{LL}$ in kV) is from 51.87 to 52.48 kV. The rated voltage of the distribution grid is 52.5 kV (1 pu). Hence, the change in the voltage at the Gse-50 50 kV substation in terms of pu quantities is within 0.988–0.99 pu. The change in the voltage phase angle ($\delta$ in degrees) at the Gse-50 50 kV substation too is hardly notable after the contingency. The changes seen are well within the grid voltage limits of 1.05 and 0.95 pu indicating no voltage stability issues within the distribution grid.

The PMU snapshot from Fig. 3 shows the real-time variation in total three-phase active power $P$ and reactive power $Q$ flow on the two Gse-Zrz 50 kV cable, measured at the Gse-50 50 kV substation in a time interval of around 2 min with the time instant of overhead line switching highlighted in red. From the highlighted section, the change in total power flow can be observed. The negative values of

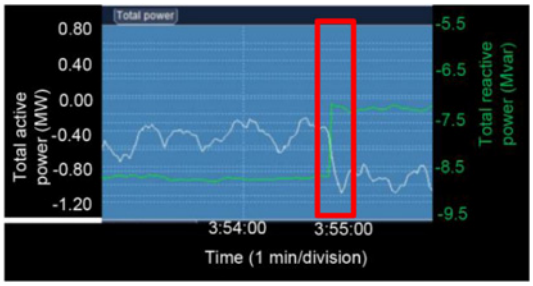


**Fig. 3** *PMU snapshot highlighting the change in active and reactive powers on the two Gse-Zrz 50 kV cable due to 50 kV overhead line disconnection*

three-phase active and reactive power ($P$ and $Q$) mean power flow into the Gse-50 50 kV substation from the two Gse-Zrz cable. The total active power flow into the Gse-50 kV substation increases from ~0.4 to 1 MW (white plot) and the total reactive power flow decreases from 8.8 to 7.4 MVAR (green plot) approximately. Identical amount of power flows into the Gse-50 50 kV substation from the one Gse-Zrz 50 kV cable connected in parallel with two Gse-Zrz 50 kV cable (see Fig. 1).

### 3.2 Contingency in 10/0.4 kV sub-distribution grid

The second contingency considered is the loss of DG from the Zrz wind farm at the Zrz 10 kV bus. Apart from the variation in the wind, which influences the power output from the wind farm, as per the inputs from the DNO Enduris, the power output from some of the DG sources is also dependent on the energy market. The case considered here is during a specific day when a controlled drop in power output from rated power of 10 MW to zero from the Zrz wind farm takes place. The sudden drop in power output is reflected as voltage oscillations and results in redistribution of power flows in the 50 kV distribution grid logged by the PMU at Zrz-50 50 kV substation as shown in Figs. 4 and 5.

Notable observations from the time instant highlighted in red in Fig. 4 are a slight drop in the per phase voltage ($V_{ph}$ in kV), approximately from 29.6 to 29.4 kV at the Zrz-50 50 kV substation. The consideration of a balanced three-phase network translates to three-phase line-to-line voltage ($V_{LL}$ in kV) from 51.3 to 51 kV (0.977 to 0.971 pu) at the Zrz-50 50 kV substation. The continuous plot of the voltage phase angle ($\delta$ in degrees) at the Zrz-50 50 kV substation shows a very small change. The changes in voltage are attributed to the sudden drop of power generation from 10 MW to zero from the wind farm at Zrz 10 kV bus.

Fig. 5 shows the real-time variation in total three-phase active power $P$ and reactive power $Q$ flowing on the Zrz-Otl-1 cable.

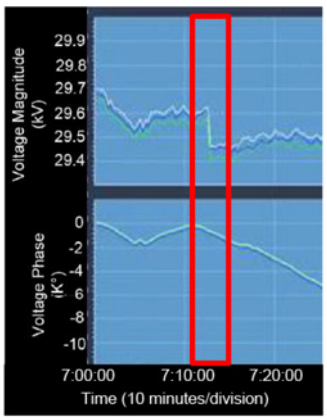


**Fig. 4** *PMU log showing the per phase voltage and instantaneous voltage phase angle at the Zrz-50 50 kV substation during sudden drop in wind power at Zrz–10 kV bus*


*CIRED, Open Access Proc. J.*, 2017, Vol. 2017, Iss. 1, pp. 1927–1930

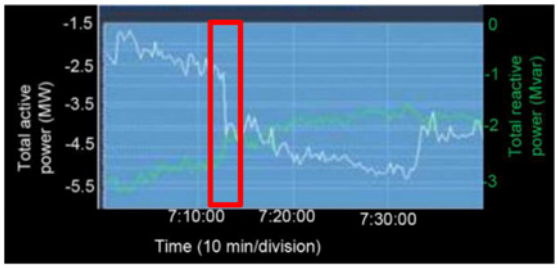


**Fig. 5** *PMU log showing the power flows on the Zrz-Otl 1 cable during sudden drop in wind power at Zrz 10 kV bus*

Notable observation from the time instant highlighted in red is the variation in total active power, which increases from ~2.9 to 4.4 MW (white plot) with a small change in the total reactive power (green plot). The negative values indicate power flowing into the Zrz-50 50 kV through the Zrz-Otl 1 cable.

Hence, from PMU logs at the Zrz-50 50 kV substation, we observe a drop in voltage and increased power flow into the Zrz-50 50 kV substation as a result of the loss of generation from the Zrz wind farm. The voltage observations show that the system remains stable, but produces slight notable voltage and power oscillations at the Zrz-50 50 kV substation.

## 4 Simulation methodology

In the simulation of both contingencies, the total aggregated values of power generation ($P_{gen}$ and $Q_{gen}$) from the DG sources (wind power and CHP plants) and the total loads ($P_L$ and $Q_L$) at each 10 kV bus is calculated separately for each contingency, since the power flow behaviour in the 50 kV grid was different during the time of each contingency. Furthermore, the actual total generation and load in the distribution grid was not available from the PMU and SCADA monitoring system during each contingency. Hence, the SCADA data was used, which provided the power exchange data between 50 and 10 kV bus. On the basis of this observed power exchange data, the total aggregated active and the reactive power generation ($P_{gen}$ and $Q_{gen}$) from DG sources at the 10 kV bus and the total aggregated load ($P_L$ and $Q_L$) at the 10 kV bus was approximately calculated, to match the pre-contingency power flow and voltages in the distribution grid. This was done separately for each of the two considered contingencies based on simple equations described below

$$P_{ex} = P_{gen} - P_L \tag{1}$$

$$Q_{ex} = Q_{gen} - Q_L \tag{2}$$

where $P_{ex}$ and $Q_{ex}$ are the active and reactive power exchange between 50 and 10 kV buses, $P_{gen}$ and $Q_{gen}$ are the aggregated active and reactive power generations at the 10 kV bus from DG sources (wind farm + CHP plants) and $P_L$ and $Q_L$ are the aggregated active and reactive power loads at the 10 kV bus.

Positive values of $P_{ex}$ and $Q_{ex}$ indicate surplus total aggregated power generation from DG sources over total aggregated load and negative $P_{ex}$ and $Q_{ex}$ values indicate that the total aggregated load is more than the total aggregated generation at each 10 kV bus. Whether there is surplus power generation or load at the 10 kV bus or not, was inferred by power flow values at each 50/10 kV transformers available from the SCADA data during the time of the two contingencies.

The time-domain-based root-mean-square analysis functionality from PowerFactory was used to separately simulate the switching out of the 50 kV overhead line and the switching out of aggregated single DFIG wind generator of 10 MW to investigate both contingencies. The results of these analyses are presented in the next section.

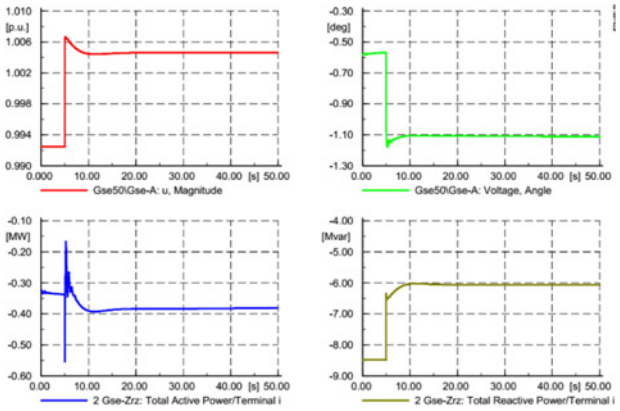


**Fig. 6** *Simulated voltage and power flow on two Gse-Zrz cable measured at Gse-50 50 kV substation (terminal i)*

## 5 Results and analysis

### 5.1 Contingency in the 50 kV distribution grid

Fig. 6 shows the results of the simulation of the first contingency. At the instant when the overhead line is switched off at 5 s, the voltage at the Gse-50 50 kV substation increases from pre-contingency value of 0.993 pu (52.13 kV) to a new steady-state value around 1.005 pu (52.7 kV). In terms of magnitude, the voltage rise is very small and within the steady-state limits of 1.05 pu indicating voltage magnitude stability. The corresponding change in voltage angle is also small. The total load at the Gse-10 10 kV bus supplied by the Gse-50 50 kV substation, although constant is modelled by voltage dependency. The slight increase in the 50 kV voltage at the Gse-50 50 kV substation is also reflected in the total active power flowing into the Gse-50 50 kV substation (terminal *i*). The part of the load is fed by Gse-Zrz 1&2 parallel cables, where the total active power flow from each 1&2 Gse-Zrz 50 kV cable is increased slightly from 0.34 MW to ~0.39 MW while the total reactive power flow decreases from 8.5 to 6 MVAR (negative values by convention mean power flow into Gse-50 50 kV substation from the two equal-impedance Gse-Zrz cables).

Disconnection of one line in the parallel line section between the Gsp-150 150 kV and Gse-50 50 kV sub-stations doubles the impedance between these substations. As a result, the total current flow decreases as observed from Fig. 7 where the shift in current flow on Zwart Gsp-Gse overhead line decreases from an initial value of 0.258 kA (twice of 0.129 kA) to a reduced value of 0.208 kA. This is accompanied by the slight reduction in the reactive power flow out of Gse-50 50 kV substation from around 22 MVAR (twice of 11 MVAR) to 17 MVAR subsequently reducing the reactive power flow on the 1&2 Gse-Zrz cables

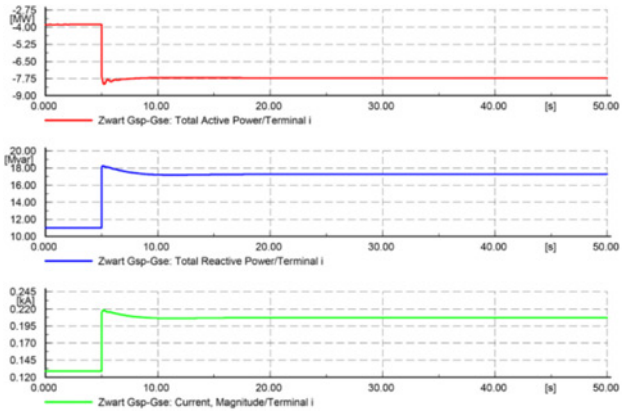


**Fig. 7** *Simulated current and power flow on Zwart Gsp-Gse 50 kV line measured at Gse-50 50 kV substation (terminal i)*

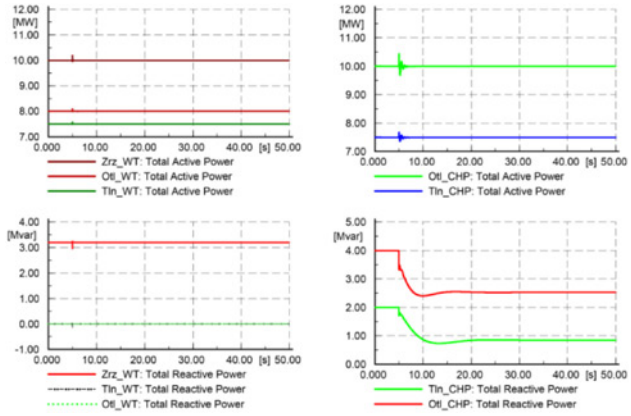


**Fig. 8** *Simulated active and reactive powers output from the DG sources*

(again, positive values indicate power flow out of the Gse-50 50 kV substation). Fig. 7 shows that the total shift of the active power flow on the Zwart Gsp-Gse 50 kV overhead line into the Gse-50 50 kV substation from 3.8 to ~7.75 MW measured at the Gse-50 50 kV substation. This power is supplied to the 50 kV distribution grid from the 150 kV transmission network represented by a slack bus.

Practically, the strong transmission network balances the power needed by the distribution grid where the 50 kV cable loadings are below 50% in this specific case. The results of power flow, current and voltages at the Gse-50 kV substation are in line with the observations from the PMU data of the contingency.

The disconnection of the 50 kV overhead line does not have any notable effects on the total supply and load demand of the distribution grid. The balancing of the distribution grid by the external slack bus (the external infinite grid connected at the Gsp-150 kV substation) means the aggregated output powers of the generators ($P_{gen}$ and $Q_{gen}$) rapidly return to their steady-state values following the disturbance as seen from Fig. 8. The change in the total reactive power supplied by the CHP generators is only affected slightly because of the action of the voltage controller.

### 5.2 Contingency in 10/0.4 kV sub-distribution grid

The second contingency concerns the switching off of the 10 MW wind generator at the Zrz 10 kV bus. The immediate observation of this event at $t = 4$ s in Fig. 9 is a drop in voltage reflected at the Zrz-10 10 kV bus and the Zrz-50 50 kV bus. The drop in voltage at Zrz-10 10 kV bus is from 1.01 pu (10.7 kV) to 0.989 pu (10.5 kV). The rated voltage of the Zrz-10 10 kV bus is 10.6 kV (1 pu). The drop in voltage at the Zrz-50 50 kV bus is from 0.992 pu (52.08 kV) to 0.986 pu (51.765 kV).

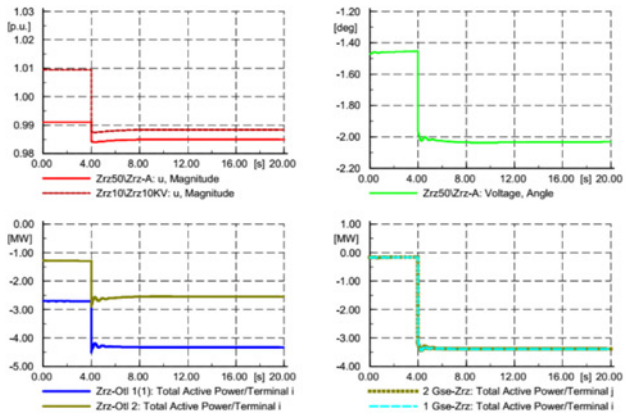


**Fig. 9** *Simulated voltages and power flow at the Zrz-50 kV substation during the second contingency*

The observed drop in voltage and voltage angle at the Zrz-10 kV and the Zrz-50 50 kV buses resulting from the loss of 10 MW generation at the Zrz 10 kV bus is marginal and within the system voltage stability limits of 1.05 and 0.95 pu, respectively. Furthermore, from Fig. 9 an increase is observed in the total active power flow into the Zrz-50 50 kV from the corresponding 50 kV cables (negative values mean power flow into the Zrz-50 50 kV bus) to meet the total load demand at the Zrz-10 kV bus as a result of loss of 10 MW generation.

The total load requirement is met collectively by the slightly increased total active power flow from Otl-50 50 kV substation having surplus power generation over load at that time instance. The rest of the active power requirement is balanced by the infinite grid of the 150 kV transmission network, which contributes a higher percentage of active power necessary for power balancing. The results from the simulation analysis compare very well with the PMU measurements at the Zrz substation.

Finally, the response of the DG sources is similar to what is seen during the first contingency in Fig. 8, with the total active power output of the generators (wind + CHP) at the 10 kV buses very quickly returning to steady-state values following the disturbance. The surplus power flow from the Otl-10 10 kV side and external grid has enough capacity to balance the power loss without significantly affecting the power output from the DG at the 10 kV sub-distribution levels.

## 6 Conclusion

The strong rise of distributed renewable energy generation has increased the need for real-time monitoring of distribution grids. In the Enduris 50 kV grid, PMU monitoring has significantly enhanced the observability of grid voltages and power flow behaviour. The analysis of the grid behaviour for two contingencies in the grid as given in this paper has proved the added value of the real-time PMU monitoring system.

From the observed PMU data and the simulations, it is concluded that the occurrence of both contingencies resulted in slight changes in voltages and redistribution of power flow in the distribution grid. The voltage fluctuations were well within the stable operating limits. A possible explanation for this is the connection of the Enduris 50 kV ring distribution grid to a secure 150 kV transmission network. The transmission network also ensures the power balancing of the distribution grid in both cases without having a significant impact on the response of the DG.

Finaly, the research described in this paper has yielded a better understanding of the Enduris distribution grid behaviour based on the analysis of actual monitored data from the PMU monitoring system. The work done supports the overall Enduris-Van Swinden Laboratory (VSL) project described in [1] aimed at efficient and effective management of the 50 kV distribution grid using PMU technology.

## 7 Acknowledgments

This work was part of the EURAMET ENG63 project, supported by the European Metrology Research Program (EMRP), which is jointly funded by the EMRP participating countries within EURAMET and the European Union.

## 8 References

1 Rietveld, G., Jongepier, A., Van Seters, J., *et al.*: 'Application of PMUs for monitoring a 50 kV distribution grid', Proc. 23rd CIRED Conference, Lyon, France, 2015, pp. 1–5
2 'DIgSILENT power factory user manual', Version 15, 2015
3 'DIgSILENT power factory application guide – DFIG template', 2015
4 Kundur, P., Balu, N.J., Lauby, M.G.: 'Power system stability and control', vol. 7 (McGraw-Hill, New York, 1994)
5 Karaliolios, P., Ishchenko, A., Coster, E., *et al.*: 'Overview of short-circuit contribution of various distributed generators on the distribution network', 43rd Int. Universities Power Engineering Conf. (UPEC), 2008, pp. 1–6